**Supplementary Information**

# Probing Side Chain Dynamics in Proteins by the Measurement of Nine Deuterium Relaxation Rates Per Methyl Group

Xinli Liao,[†,‡] Dong Long,[§] Da-Wei Li,[§] Rafael Brüschweiler,[§] and Vitali Tugarinov[‡,*]

[‡]*Department of Chemistry and Biochemistry, University of Maryland, College Park, Maryland 20742, and* [§]*Chemical Sciences Laboratory, Department of Chemistry and Biochemistry and the National High Magnetic Field Laboratory, Florida State University, Tallahassee, Florida 32306*

**Simulations of $R_2$(CHD$_2$) Decay in ($^{13}$CH)D$_2$ Methyl Groups.** Relaxation of $^2$H single-quantum transitions in ($^{13}$CH)D$_2$ methyl groups $\rho_{i\text{-}j}$ (Figure 2 of the main text) can be conveniently represented in the following form,

$$\frac{d}{dT}\begin{bmatrix}\rho_{1-2}\\ \rho_{2-3}\\ \rho_{3-4}\\ \rho_{4-5}\\ \rho_{5-6}\\ \rho_{6-7}\end{bmatrix} = -\left(\frac{1}{80}\right)(2\pi QCC)^2 \left[\begin{pmatrix}9&0&0&0&0&0\\0&9&0&0&0&0\\0&0&9&0&0&0\\0&0&0&9&0&0\\0&0&0&0&9&0\\0&0&0&0&0&9\end{pmatrix} J^A(0) + \begin{pmatrix}15&-\sqrt{6}&0&0&3\sqrt{2}&0\\-\sqrt{6}&19&1&0&0&-3\sqrt{3}\\0&1&19&-\sqrt{6}&3\sqrt{3}&0\\0&0&-\sqrt{6}&15&0&3\sqrt{2}\\3\sqrt{2}&0&3\sqrt{3}&0&15&3\\0&-3\sqrt{3}&0&3\sqrt{2}&3&15\end{pmatrix} J^A(\omega_D) \right.$$
$$+ \begin{pmatrix}6&-\sqrt{6}&0&0&-3\sqrt{2}&0\\-\sqrt{6}&-2&1&0&0&3\sqrt{3}\\0&1&-2&-\sqrt{6}&3\sqrt{3}&0\\0&0&-\sqrt{6}&6&0&-3\sqrt{2}\\-3\sqrt{2}&0&3\sqrt{3}&0&-6&3\\0&3\sqrt{3}&0&-3\sqrt{2}&3&-6\end{pmatrix} J^C(\omega_D)$$
$$+ \begin{pmatrix}18&0&-2\sqrt{6}&0&0&-6\sqrt{2}\\0&10&0&-2\sqrt{6}&0&0\\-2\sqrt{6}&0&10&0&0&0\\0&-2\sqrt{6}&0&18&-6\sqrt{2}&0\\0&0&0&-6\sqrt{2}&18&0\\-6\sqrt{2}&0&0&0&0&18\end{pmatrix} J^A(2\omega_D)$$
$$\left. + \begin{pmatrix}0&0&-2\sqrt{6}&0&0&6\sqrt{2}\\0&4&0&-2\sqrt{6}&0&0\\-2\sqrt{6}&0&4&0&0&0\\0&-2\sqrt{6}&0&0&6\sqrt{2}&0\\0&0&0&6\sqrt{2}&-12&0\\6\sqrt{2}&0&0&0&0&-12\end{pmatrix} J^C(2\omega_D) \right] \begin{bmatrix}\rho_{1-2}\\ \rho_{2-3}\\ \rho_{3-4}\\ \rho_{4-5}\\ \rho_{5-6}\\ \rho_{6-7}\end{bmatrix}$$

where $QCC$=($e^2qQ/h$) is a quadrupolar coupling constant (167 kHz[1]) and $J(\omega)$ is the spectral density function,[2-4]

$$J(\omega) = \frac{1}{9}S^2_{axis}\left(\frac{\tau_C}{1+(\omega\tau_C)^2}\right) + \left(P_2(\cos\alpha) - \frac{1}{9}S^2_{axis}\right)\frac{\tau_e}{1+(\omega\tau_e)^2} \qquad \text{(S1)}$$

where $S^2_{axis}$ is the generalized order parameter of the methyl 3-fold symmetry axis; $P_2 = (1/2)[3\cos^2(x)-1]$; $\alpha$=0° and $P_2(\cos\alpha) = 1$ for the auto-correlation spectral density function, $J^A(\omega)$, while $\alpha = 109.5°$ and $P_2(\cos\alpha) = -1/3$

for the quadrupolar cross-correlation spectral density, $J^C(\omega)$; $\tau_C$ is the (isotropic) correlation time of overall molecular re-orientation; $1/\tau_e = 1/\tau_f + 1/\tau_C$ where $\tau_f$ is the correlation time of fast local motions.

Simulations of the transverse magnetization decay in ($^{13}$CH)$D_2$ groups, $R_2(CHD_2)$, have been performed using the matrix exponential of the matrices in eqs S1 expanded to include the triple-quantum (3Q) terms present during relaxation delay $T$, $(\rho_{1-4}^{3Q} + \rho_{2-5}^{3Q})$ (see expression 5 of the main text). The following initial conditions for $\rho_{i\text{-}j}$ have been used:

$\rho(0) = (1/9)\left[\sqrt{F_1}\rho_{1-2}; \sqrt{F_2}\rho_{2-3}; \sqrt{F_2}\rho_{3-4}; \sqrt{F_1}\rho_{4-5}; \sqrt{F_3}\rho_{5-6}; \sqrt{F_3}\rho_{6-7}; \sqrt{F_{3Q}}(\rho_{1-4}^{3Q} + \rho_{2-5}^{3Q})\right]^T$, where

$F_i$ is the 'out-and-back' transfer function of each individual transition in the experiment of Figure 1 of the main text, and superscript $T$ denotes the transposition operation. From expression (5) of the main text it follows that:

$$F_1 = 0.25\left[2\sin\left(4\pi J_{CD}T_C\right) + \sin\left(8\pi J_{CD}T_C\right)\right]^2 \quad \text{(S2a)}$$

$$F_2 = 1.5\sin^2\left(8\pi J_{CD}T_C\right) \quad \text{(S2b)}$$

$$F_3 = 2\sin^2\left(4\pi J_{CD}T_C\right) \quad \text{(S2c)}$$

$$F_{3Q} = \left[0.5\sin\left(8\pi J_{CD}T_C\right) - \sin\left(4\pi J_{CD}T_C\right)\right]^2 \quad \text{(S2d)}$$

The sum of all transfer functions in eqs S2 above gives $4\sin^2\left(4\pi J_{CD}T_C\right) + 2\sin^2\left(8\pi J_{CD}T_C\right)$ - the transfer function used for the sum of *all* transitions relaxing during the delay $T$ in the experiment for $R_2(CHD_2)$ measurement (Figure 1, inset ***A***). To account for the differential transfer efficiency of $\rho_{i\text{-}j}$ in the reverse pathway of the scheme, after the relaxation period $T$ each of the transitions has been pre-multiplied by its corresponding $\sqrt{F_i}$ before summation. Note the scaling of $\rho(0)$ as above ensures that the sum of all transitions at $T = 0$ is normalized to unity.

Thus simulated $R_2(CHD_2)$ decays have been fitted to a single-exponential function $I = I_0\, exp(-RT)$, where $I$ is the simulated intensity and $R$ is the relaxation rate. The results of these simulations expressed as relative errors in $R_2(CHD_2)$ arising from non-single-exponential decay at higher frequencies, $100*R_2(CHD_2)$-$R(D_+,CH_2D))/R(D_+,CH_2D)$, are illustrated in Figure 4 of the main text for several global molecular correlation times.

**Figure S1**

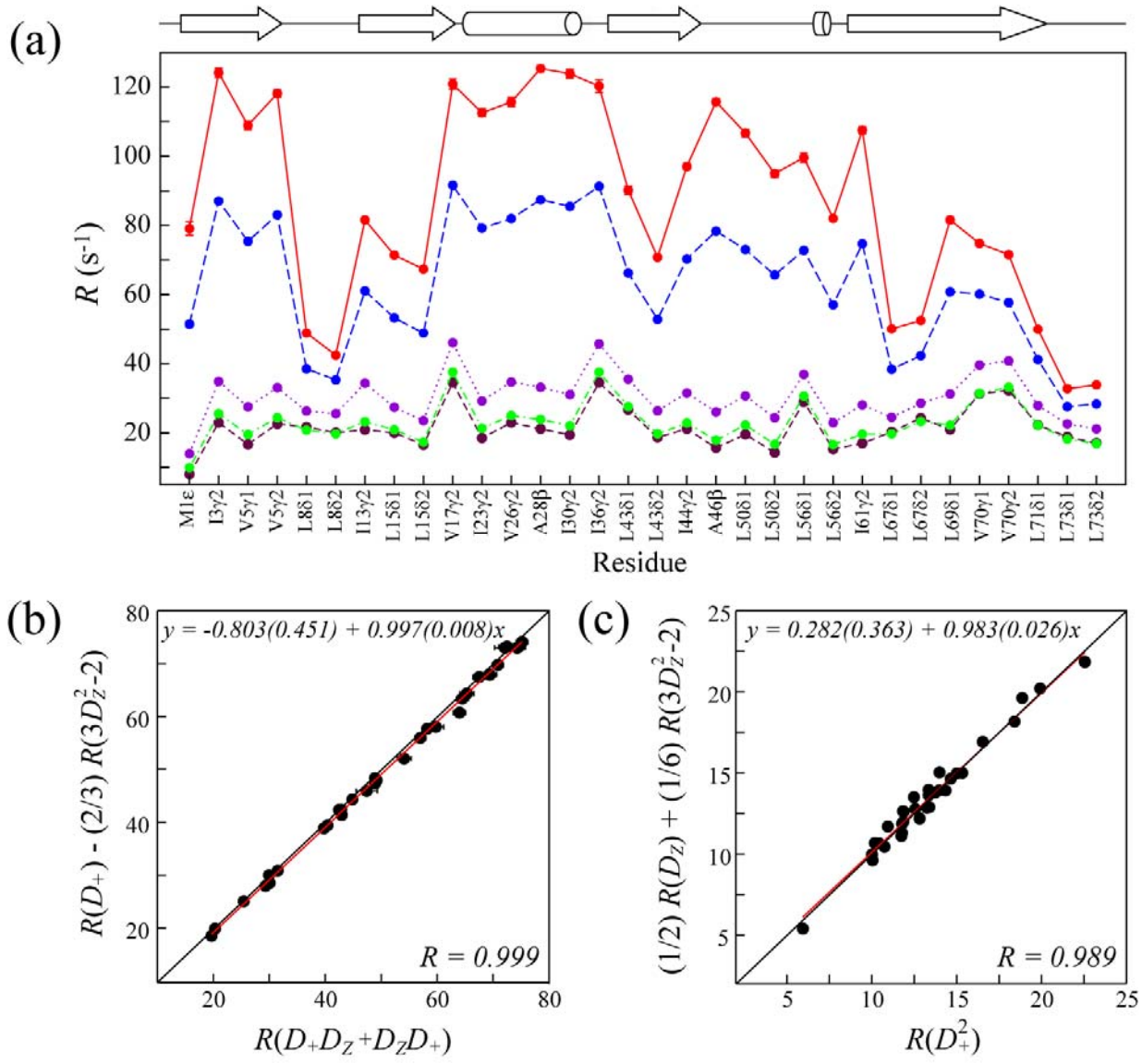


***Figure S1.*** **(a)** All $^{2}$H relaxation rates measured in $^{13}CH_2D$ methyl groups of ubiquitin at 27 °C satisfy the consistency relations. **(a)** $(5/3)R(D_+D_Z+D_ZD_+) \geq R(D_+) \geq (5/3)R(3D_Z^2\text{-}2) \geq (5/3)R(D_+^2) \geq R(D_Z)$. The rates $(5/3)R(D_+D_Z+D_ZD_+)$, $(5/3)R(D_+)$, $R(3D_Z^2\text{-}2)$, $(5/3)R(D_+^2)$ and $R(D_Z)$ are shown with red, blue, purple, green and brown circles/lines, respectively, *vs.* methyl positions; **(b-c)** Linear correlation plots of **(b)** $R(D_+D_Z+D_ZD_+)$ rates (*x*-axis) *vs.* $R(D_+) - (2/3)R(3D_Z^2\text{-}2)$ (*y*-axis), and **(c)** $R(D_+^2)$ (*x*-axis) *vs.* $(1/2)R(D_Z) + (1/6)R(3D_Z^2\text{-}2)$ (*y*-axis) for 32 methyl groups in ubiquitin.

**Figure S2**

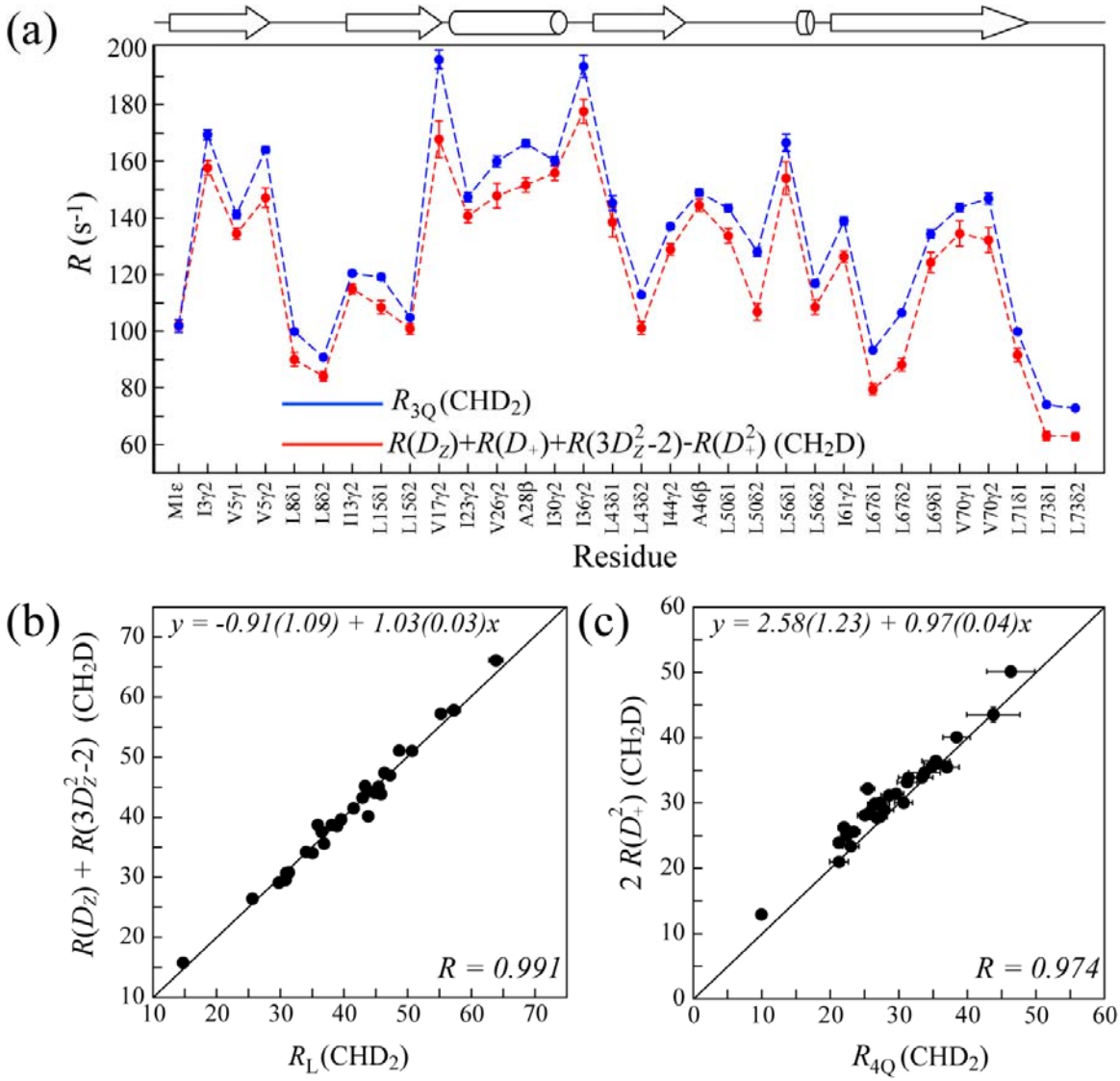


***Figure S2.*** **(a)** All $^{2}$H relaxation rates measured in $^{13}CHD_2$ methyl groups of ubiquitin at 10 °C satisfy the consistency relations. **(a)** $R_{3Q}(CHD_2) \leq R(D_Z)+R(D_+)+R(3D_Z^2\text{-}2)\text{-}R(D_+^2)$ ($CH_2D$) (shown with red and blue circles/lines, respectively, *vs.* methyl position). **(b-c)** Linear correlation plots of **(b)** $R_L(CHD_2)$ rates (*x*-axis) *vs.* $R(D_Z) + R(3D_Z^2\text{-}2)$ ($CH_2D$) (*y*-axis) and **(c)** $R_{4Q}$ ($CHD_2$) (*x*-axis) *vs.* $2R(D_+^2$; $CH_2D$) (*y*-axis) for 29 methyl groups of ubiquitin. Three residues with large errors in the measurements (> 6 %) have been eliminated from the plots in (b-c).

**Figure S3**

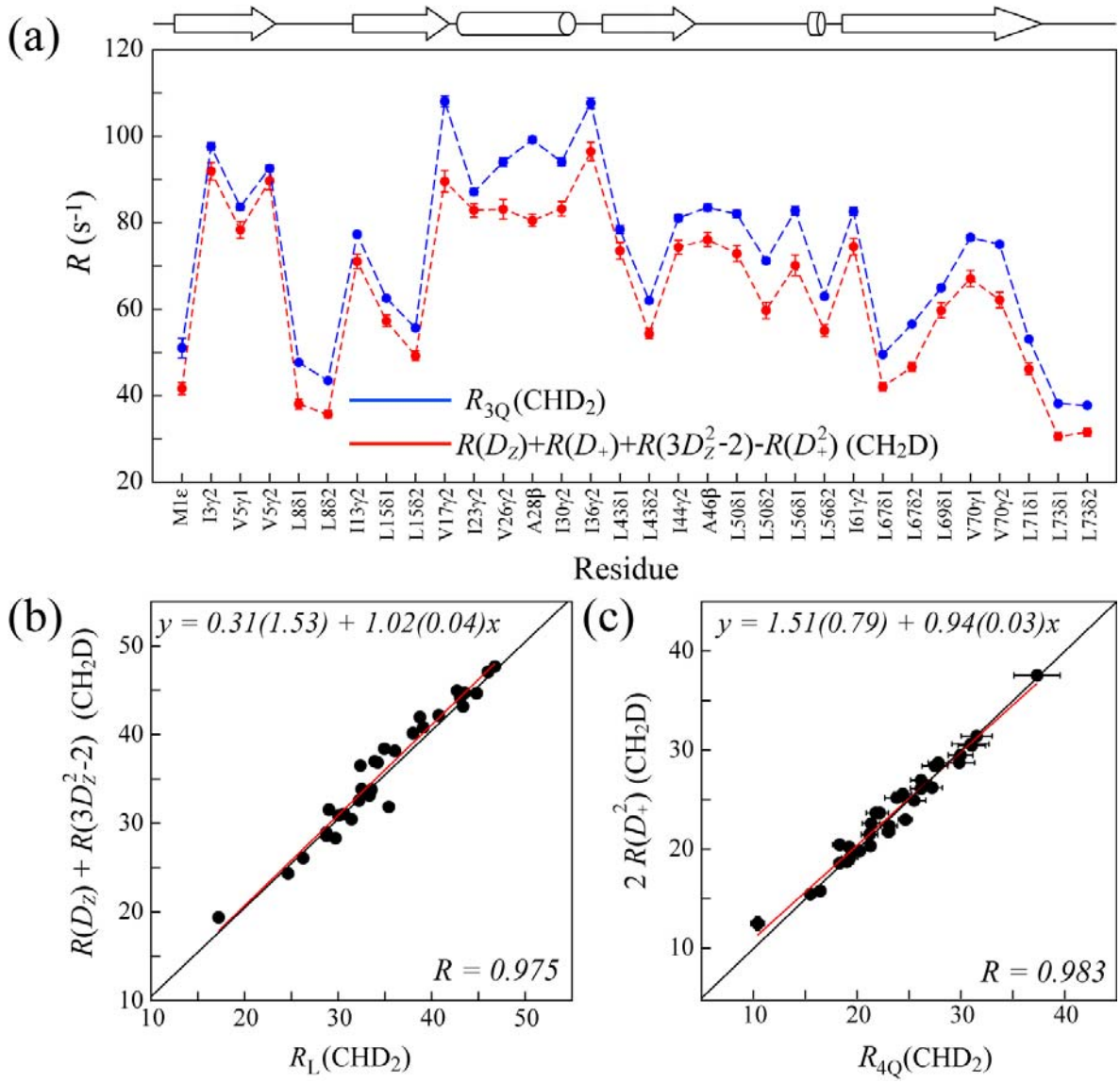


***Figure S3.*** **(a)** All $^{2}$H relaxation rates measured $^{13}CHD_2$ methyl groups of ubiquitin at 40°C satisfy the consistency relations. **(a)** $R_{3Q}(CHD_2) < R(D_Z)+R(D_+)+R(3D_Z^2\text{-}2)\text{-}R(D_+^2)$ ($CH_2D$) (shown with red and blue circles/lines, respectively *vs.* methyl position). **(b-c)** Linear correlation plots of **(b)** $R_L(CHD_2)$ rates (*x*-axis) *vs.* $R(D_Z) + R(3D_Z^2\text{-}2)$ ($CH_2D$) (*y*-axis) and **(c)** $R_{4Q}$ ($CHD_2$) (*x*-axis) *vs.* $2R(D_+^2$; $CH_2D$) (*y*-axis) for 31 methyl groups in ubiqutin. 1 residue has been eliminated from the plots in (b-c) due to very high errors in the extracted relaxation rates.

**Figure S4**

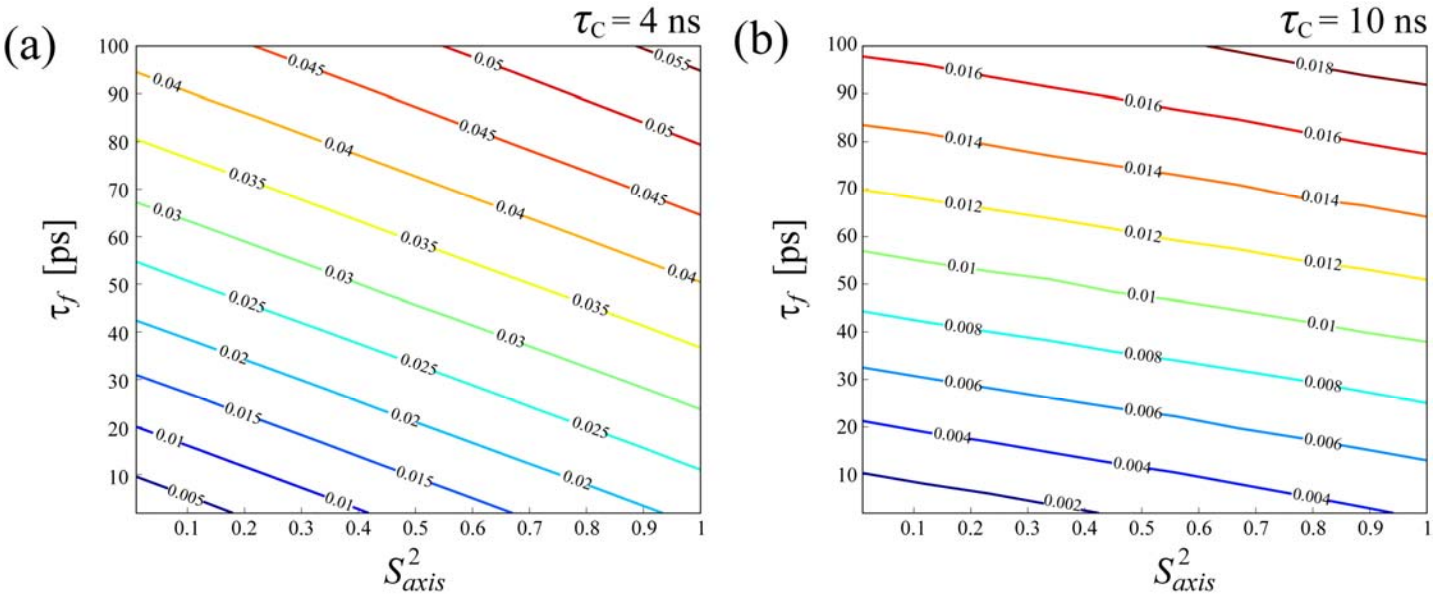


***Figure S4.*** Contour plots showing simulated absolute differences between synthetic-[$R_L$; $R_2(CHD_2)$]-derived and input $S^2_{axis}$ values ($S^2_{axis}(CHD_2)$ - $S^2_{axis}$) as a function of ($S^2_{axis}$; $\tau_f$) for the global isotropic molecular reorientation correlation times ($\tau_C$) of **(a)** 4 ns; **(b)** 10 ns. The $R_2(CHD_2)$ rates have been simulated as described in the Supporting Information and best-fit to $R(D_+;CH_2D)$ = $(1/80)(2\pi QCC)^2[9J(0) + 15J(\omega_D) + 6J(2\omega_D)]$, while $R_L(CHD_2)$ have been fit to $(3/40)(2\pi QCC)^2[4J(\omega_D) + 4J(2\omega_D)]$ = $R(3D_Z^2\text{-}2; CH_2D) + R(D_Z; CH_2D)$.

**Figure S5**

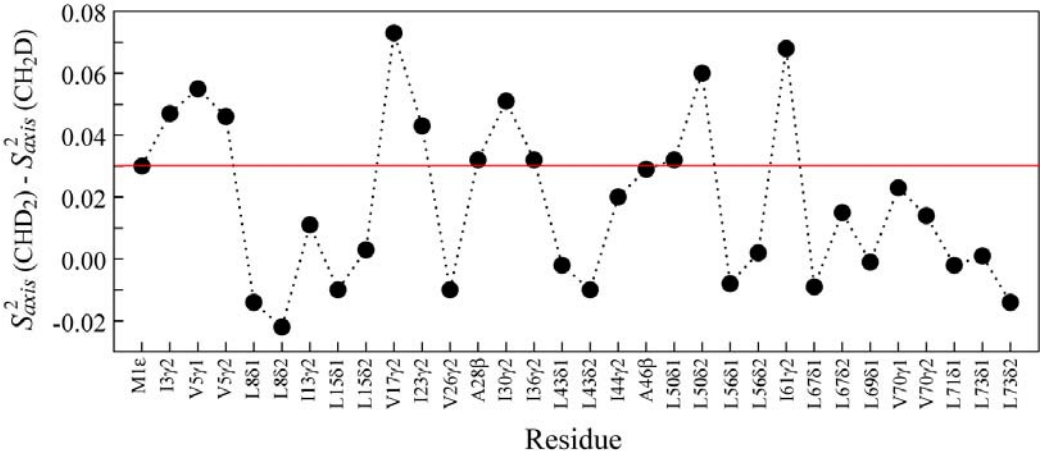


***Figure S5.*** The differences between the [$R_2$, $R_L(CHD_2)$]-derived and [$D_+$, $D_Z(CH_2D)$]-derived $S^2_{axis}$ values in ubiquitin at 40°C [$S^2_{axis}(CHD_2)$ - $S^2_{axis}(CH_2D)$] plotted versus methyl-containing residue numbers. The approximate position of the average absolute deviation [$S^2_{axis}(CHD_2)$ - $S^2_{axis}(CH_2D)$] predicted from simulations for $\tau_C$ = 4 ns is shown with horizontal red line.

**Figure S6**

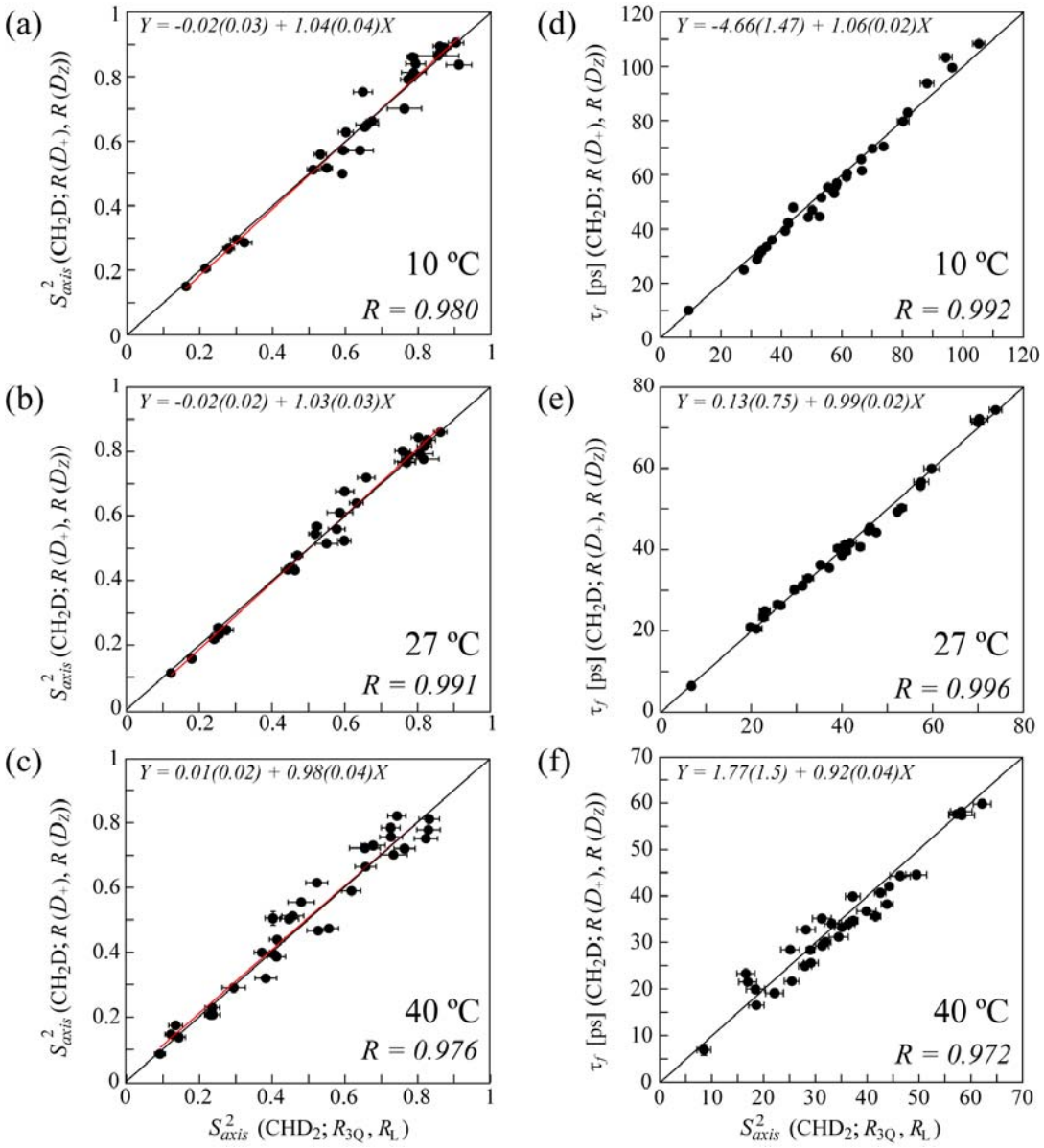


***Figure S6.*** Linear correlation plots of **(a-c)** [$R_{3Q}$,$R_L$(CHD$_2$)]-derived $S^2_{axis}$ ($x$-axis) *vs.* [$R(D_+,D_Z$; CH$_2$D)]-derived $S^2_{axis}$ ($y$-axis) at 10, 27 and 40°C; **(d-f)** [$R_{3Q}$,$R_L$(CHD$_2$)]-derived $\tau_f$ values ($x$-axis) *vs.* [$R(D_+,D_Z$; CH$_2$D)]-derived $\tau_f$ ($y$-axis) at 10, 27 and 40°C. Linear regression parameters are shown for each plot along with Pearson correlation coefficients, $R$. Solid diagonal lines correspond to $y = x$.

**Figure S7**

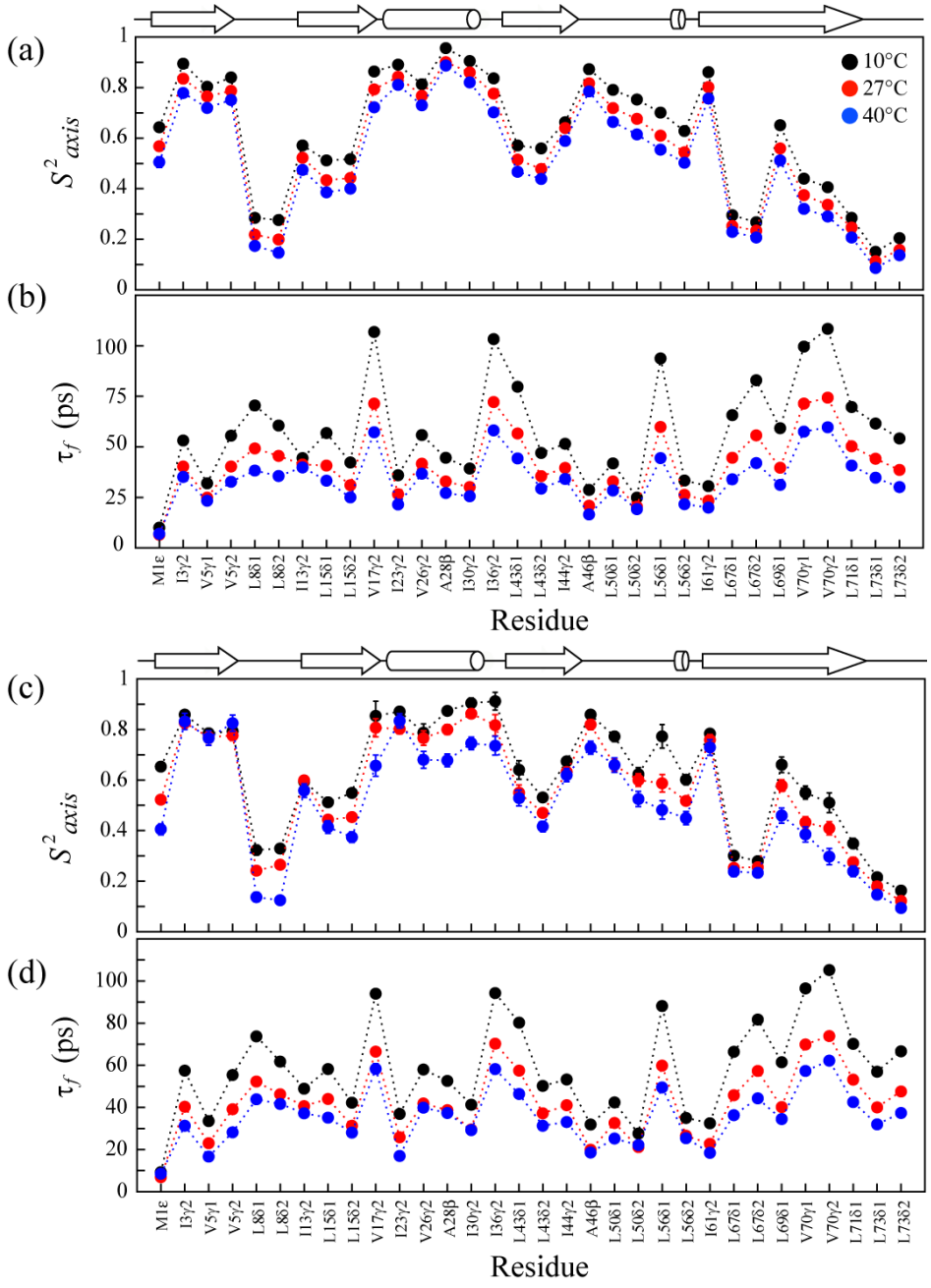


***Figure S7.*** Comparisons of $S^2_{axis}$ and $\tau_f$ values obtained for 32 methyl groups of ubiquitin at 10°C (black circles), 27°C (red circles) and 40°C (blue circles): **(a)** **[**$R(D_+,D_Z$; $CH_2D)$]-derived $S^2_{axis}$, **(b)** [$R(D_+,D_Z$; $CH_2D)$]-derived $\tau_f$ values (ps); **(c)** **[**($R_{3Q}$,$R_L$; $CHD_2$)]-derived $S^2_{axis}$ and **(d)** [($R_{3Q}$,$R_L$; $CHD_2$)]-derived $\tau_f$ values.

**Figure S8**

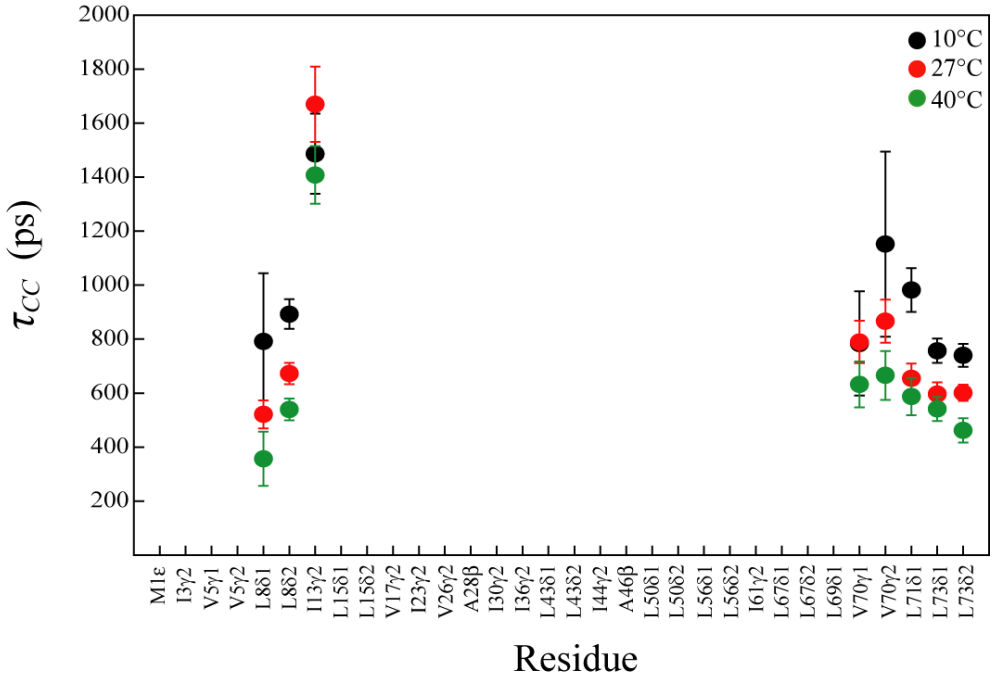


***Figure S8.*** Temperature dependence of the time-scales of slow methyl axis motions/rotameric jumps ($\tau_{CC}$; ps) for the subset of methyl groups of ubiquitin that have statistically significant reduction in reduced $\chi^2$ when five $^2$H relaxation rates (see main text) are best-fit to the spectral density function in eq. 2b. The values of $\tau_{CC}$ are shown at 10°C (black circles), 27°C (red circles) and 40°C (green circles).

**Supplementary References**


(1) Mittermaier, A.; Kay, L. E. *J. Am. Chem. Soc.* **1999**, *121*, 10608.

(2) Lipari, G.; Szabo, A. *J. Am. Chem. Soc.* **1982**, *104*, 4559.

(3) Woessner, D. E. *J. Chem. Phys.* **1962**, *37*, 647.

(4) Skrynnikov, N. R.; Millet, O.; Kay, L. E. *J. Am. Chem. Soc.* **2002**, *124*, 6449.